Deglacial ice sheet instabilities induced by proglacial lakes

Aurélien, Quiquet[1], Christophe, Dumas[1], Didier, Paillard[1],Gilles, Ramstein[1], Catherine, Ritz[2], Didier M., Roche[1,3]

[1]Laboratoire des Sciences du Climat et de l'Environnement, LSCE/IPSL, CEA-CNRS-UVSQ, Université Paris-Saclay, F-91191 Gif-sur-Yvette, France
[2]Université Grenoble Alpes, CNRS, IRD, Grenoble INP, IGE, 38000 Grenoble, France
[3]Vrije Universiteit Amsterdam, Faculty of Science, Cluster Earth and Climate, de Boelelaan 1085, 1081HV Amsterdam, The Netherlands

Key Points:

- The North American proglacial lakes induce an ice sheet instability during the last deglaciation
- This mechanical instability could explain half of the mass loss for the final stage of the North American ice sheet
- This mechanism could provide a physical origin for the debated melt water pulse 1B

Corresponding author: Aurélien Quiquet, `aurelien.quiquet@lsce.ipsl.fr`

Abstract

During the last deglaciation (21 - 7 kaBP), the gradual retreat of Northern Hemisphere ice sheet margins produced large proglacial lakes. While the climatic impacts of these lakes have been widely acknowledged, their role on ice sheet grounding line dynamics has received very little attention so far. Here, we show that proglacial lakes had dramatic implications for the North American ice sheet dynamics through a self-sustained mechanical instability which has similarities with the known marine ice sheet instability albeit providing fast retreat of large portions of the ice sheet over the continent. Systematically reproduced in the latest stage of the deglaciation, this mechanism could provide a physical origin for the debated melt water pulse 1B. Echoing our knowledge of Antarctic ice sheet dynamics, they are another manifestation of the importance of grounding line dynamics for ice sheet evolution.

Plain Language Summary

While ice sheet contribution to future sea level rise remains uncertain, the last deglaciation provide an unique opportunity to understand the mechanisms behind large-scale ice sheet collapses. In recent years, ice sheet models have substantially improved as they now better represent ice dynamics than they used to. Here we use such a model to quantify for the first time the importance of proglacial lakes on ice sheet dynamics. We show that these lakes could be responsible for large-scale ice sheet collapses due to a flotation instability. The proglacial lake ice sheet instability could be an additional mechanism explaining observed late deglacial melt water pulses.

1 Introduction

Proglacial lakes have formed, evolved and drained in response to ice sheet changes throughout the Pleistocene (Teller, 1995). These lakes form at an ice margin by ice and/or moraine damming or in depressed basins. During the last deglaciation (21 - 7 kaBP), these lakes were a common feature of the Northern Hemisphere landscape, spanning a range of sizes reaching up several thousands of square kilometres in extent (Carrivick & Tweed, 2013). These lakes can be short-lived or last for several thousand years and may experience abrupt changes in water level (Teller & Leverington, 2004). These abrupt water level drops have sometimes resulted in large lake outbursts that probably had important consequences on the global climate owing to the large resulting freshwater flux to the oceans (Teller & Leverington, 2004). It is widely acknowledged, for example, that the abrupt drainage at 8.2 kaBP of Lake Agassiz-Ojibway, the largest known lake on Earth, which existed for thousands of years, induced a widespread cooling of the Northern Hemisphere via a slowdown of the Atlantic circulation (Barber et al., 1999; Wiersma & Renssen, 2006). Proglacial lakes have also had an impact at the regional scale, in particular for ice sheet surface mass balance, reducing summer ablation and favouring ice growth (Hostetler et al., 2000; Krinner et al., 2004). As the climatic importance of these lakes is well established, it is surprising perhaps that their role in ice sheet mechanics has received very little attention so far. Yet, using conceptual models for ice ages, some authors have hypothesised that these lakes could be responsible for Pleistocene ice volume oscillations, favouring calving and thus enhancing rapid ice retreat (Pollard, 1982; Fowler et al., 2013). This hypothesis has hitherto been tested with comprehensive physically-based numerical ice sheet models. Here, we use a set of numerical model experiments to study the impact of large proglacial lakes on ice sheet grounding line dynamics and to quantify their potential contribution to sea level rise accelerations during the last deglaciation.

Sea-level archives suggest that the deglacial rate of sea level rise has been far from linear, with episodic rapid accelerations (Lambeck et al., 2014). Amongst these events, the melt water pulse 1A (MWP-1A) is the most prominent feature with 14 to 18 metres of sea level rise in 340 years between 14.65 kaBP and 14.31 kaBP (Deschamps et al., 2012).

Later in the deglaciation, between 11.45 kaBP and 11.1 kaBP, another event, the melt water pulse 1B (MWP-1B), could also have been as large as about 14 metres over 350 years (Abdul et al., 2016) even if its existence is controversial due to its absence in some archives (Bard et al., 2016). These events suggest large-scale ice sheet collapses. So far, our understanding of the underlying processes leading to such ice sheet collapses is limited.

If there is no consensus on the geographic origin of the freshwater outbursts during these events (Liu et al., 2016) the comprehensive glacial histories of ICE-6G_C (Peltier et al., 2015) and GLAC-1D (Tarasov et al., 2012; Ivanovic et al., 2016), derived from inversion of indicators for modern surface subsidence measurements and past relative sea level evolution (supporting information Text S2), both suggest that the North American ice sheet (NAIS) was probably an important contributor to the MWP-1A with a rate of volume change of about 3 m of global sea level equivalent (mSLE) per century. Towards the end of the Younger Dryas, GLAC-1D also presents a collapse of this ice sheet at a rate of 1.5 mSLE per century. Although this feature of the late deglacial NAIS is absent from ICE-6G_C, using the same glacial isostatic data but including an updated ice sheet model, a recent study (Stuhne & Peltier, 2017) has also suggested that a collapse of the late deglacial NAIS could explain the MWP-1B.

Several mechanisms could explain these large scale ice sheet collapses: i) ice stream surges due to internal thermo-mechanical oscillations (MacAyeal, 1993; Calov et al., 2002); ii) grounding line migration for marine ice sheets (DeConto & Pollard, 2016); or iii) strongly negative surface mass balance due to the surface elevation feedbacks (Gregoire et al., 2012; Abe-Ouchi et al., 2013). To date, only this last process has been used in a modelling study to successfully reproduce the largest deglacial abrupt sea level rise, the MWP-1A, with a so-called saddle collapse mechanism (Gregoire et al., 2012). Surface mass balance processes such as the saddle collapse are enhanced by abrupt warming such as the Bølling-Allerød that was mostly synchronous with the MWP-1A. Unlike surface mass balance processes, once triggered, mechanical instabilities are self-sustained and are only weakly sensitive to any later climate change.

Whilst a fair amount of ice sheet simulations of Northern Hemisphere deglaciation are available in the literature, they were performed with a former generation of ice sheet models that do not account for the complexity of grounding line dynamics (Gregoire et al., 2012; Abe-Ouchi et al., 2013; Charbit et al., 2005; Heinemann et al., 2014; Ganopolski & Brovkin, 2017). Ice sheet models now either use a very high spatial resolution at the ice margin to explicitly solve grounding line dynamics (Larour et al., 2012), in some cases with some sub-grid parametrisations (Winkelmann et al., 2011), or they impose an ice flux crossing the grounding line using analytically derived formulations (Schoof, 2007; Tsai et al., 2015). These newer models have a grounding line migration that is much more sensitive to changes in boundary conditions (mass balance and sea level (Pattyn et al., 2013)) with respect to the previous generation.

2 Methods

In this work, we use the GRISLI ice sheet model (Quiquet, Dumas, et al., 2018) to simulate the evolution of the Northern Hemisphere ice sheets for the last 26 ka. We showed recently that the model was able to correctly reproduce the grounding line migration for the Antarctic ice sheet across the last glacial-interglacial cycles (Quiquet, Dumas, et al., 2018). The ice sheet model accounts for glacial isostasy with an elastic lithosphere - relaxed asthenosphere model. Any topographic depression below the contemporaneous eustatic sea level is assumed to be flooded with a water surface elevation at the eustatic sea level value. The climatic forcing that drives the ice sheet evolution is computed in two completely independent ways. In a first series of experiments the iLOVECLIM climate model (Roche, Dumas, et al., 2014; Roche, Paillard, et al., 2014) is bi-directionally coupled to GRISLI using a new downscaling capability (Quiquet, Roche, et al., 2018) to compute ice sheet surface mass balance from downscaled physical variables at the resolution of the ice sheet model for each atmospheric model time step. Surface mass balance is computed with an insolation - melt model (van den Berg et al., 2008) with local melt parameter tuning to partially correct for the model biases (Heinemann et al., 2014). Sub-shelf melting rate is computed from temperature and salinity provided by the ocean model (Beckmann & Goosse, 2003). The second series of experiments consist of a suite of ice sheet stand-alone experiments forced by an ensemble of synthetic climate histories that are elaborated from general circulation model (GCM) outputs and a proxy for temperature variability deduced from a Greenland ice core (Charbit et al., 2007). In this case, the GCM last glacial maximum anomalies with respect to the pre-industrial from the PMIP3 database (Abe-Ouchi et al., 2015) are added to reanalysis data (Dee et al., 2011). If these stand-alone experiments use an idealised climate forcing that may lack consistency between ice sheet and climate changes, they nonetheless provide an ensemble of alternative ice sheet evolutions during the deglaciation. More details on the modelling setup is given in the supporting information (Text S1).

3 Results

Both sets of experiments produce deglacial NAIS volume losses in general agreement with the geologically-constrained reconstructions (Fig. 1A). However, in detail they do present some important differences. On the one hand, the stand-alone experiments show a pronounced millenial scale variability in ice volume, which is a direct consequence of the imposed atmospheric variability recorded in Greenland ice cores. In particular, the simulated NAIS loses ice up to a rate of 5 mSLE per century (Fig. 1B) in response to the abrupt Bølling warming at 14.6 kaBP. That rate is comparable to the magnitude of the MWP-1A recorded in sea-level archives (Deschamps et al., 2012). These experiments show a second maximum in rate of volume loss towards the end of the Younger Dryas circa 11.5 kaBP, in agreement with the GLAC-1D reconstruction. On the other hand, in the coupled experiment, the gradual change in forcings (orbital and greenhouse gases) leads to a smoother simulated ice volume reduction. While ice volume between 26 and 17 kaBP is relatively stable, after this date, the ice loss rates are overestimated with respect to the geomorphological reconstructions, leading to a smaller simulated ice sheet extent (Fig. S1 and Fig. S2). This faster ice sheet volume reduction in the coupled experiment is in part due to the fact that we do not account for the impact of melt water flux to the ocean which are expected to weaken the North Atlantic overturning circulation and, as a result, to delay the Northern Hemisphere warming. Since the coupled model does not internally produce the Bølling warming, contrary to the stand-alone experiments, it presents only one peak in rates of volume loss circa 13 kaBP of about 2 mSLE per century. We show in the following that the latest acceleration in ice loss, in the two sets of experiments, is due to the large proglacial lake that forms at the southern edge of the NAIS.

The pattern of our modelled NAIS retreat in the coupled experiment is illustrated in Fig. 2 with two selected snapshots; one before and one after the timing of maximum ice loss rate for the coupled experiment. At 13.8 kaBP (before the event, Fig. 2A), the simulated ice sheet reproduces the major ice streams inferred by geomorphological observations (Hudson Strait, Lancaster Sound, Amundsen Gulf (Margold et al., 2018) on Fig. 2). This ice streams are predominantly controlled by bedrock features (valleys, Fig. S3) and terminate in the Atlantic and Arctic oceans. On the contrary, the continental southern margin does not show at this time any well identified ice streams. However, retreat of the ice sheet on its southern margin produced the large proglacial lake Agassiz-Ojibway (Teller, 2003). One thousand years later, at 12.8 kaBP (Fig. 2B), dramatic acceleration of the southern part of the ice sheet is simulated and associated with substantial grounding line retreat. Velocities of grounded ice shift from below 500 m yr^{-1} to about 2000 m yr^{-1}

in the vicinity of the grounding line. In the stand-alone experiments this rapid acceleration in ice sheet velocity is systematically reproduced independently from the climatic forcing, but it occurs later, towards the end of the Younger Dryas (Fig. S4). This rapid ice sheet collapse is due to a mechanism similar to the marine ice sheet instability (Weertman, 1974; Schoof, 2007) except that it occurs in a lake and not in the ocean. In the following, this process will be referred to as proglacial lake ice sheet instability, PLISI.

To better illustrate the mechanism, we show a cross-section of the ice sheet for the same temporal snapshots in Fig. 3. Before the instability initiation, the bedrock under the ice sheet is depressed with respect to its present-day value due to the glacial ice load (Fig. 3A). In the course of the deglaciation, the progressive thinning due to surface mass balance decrease leads eventually to floating conditions and the retrograde bed triggers the PLISI. The grounding line retreats by more than 700 km in the region of Lake Agassiz-Ojibway within one thousand years (Fig. 3B). Once triggered, the mechanism is mostly mechanically driven (supporting information Text S3).

To assess the importance of the PLISI in shaping the deglaciation, we isolate the effect of surface mass balance by preventing the occurrence of the mechanical instability, by assuming that the southern margin of the NAIS is perpetually grounded until 8 kaBP. Excluding lake effects on ice dynamics results in maximal rates of ice loss halved with respect to the experiments in which the PLISI is accounted for (Fig. 4 and Fig. S7). In particular, magnitude of local ice fluxes are divided by 10 in the area of present-day Hudson Bay (Fig. S8). The PLISI is thus a crucial process for the NAIS dynamics and explains the late deglacial acceleration of the ice sheet volume loss.

Since the PLISI is a grounding line instability, its importance is tightly linked to the lake water depth through a flotation criteria. Our ice sheet model does not simulate explicitly proglacial lakes and the lake surface elevation is assumed to follow the eustatic sea level. This is a conservative estimate since at high latitudes the water inputs to the lake exceed the evaporation and the water level is thus controlled by the elevation of the outlet. It is believed that large proglacial lakes at the southern margin of the NAIS presented probably a surface level about 100 metres or more above the contemporaneous eustatic sea level (Lambeck et al., 2017; Clarke et al., 2004). For this reason, we performed additional experiments for which we assume a constant lake surface elevation at +50 m above present-day sea level in the NAIS southern margin area (about +120 m above eustatic sea level at 13 kaBP). In this case, the PLISI is enhanced and it often doubles the maximum ice loss rate compared to the simulations where the mechanism is inhibited (Fig. 4 and Fig. S7). While these additional experiments with a higher lake surface elevation lead to substantial difference in ice loss rates, we made additional computations that suggest that the elevation could be higher than +150 metres above present-day sea-level in the course of the deglaciation (supporting information Text S4). This implies that if more realistic varying lake surface elevations were considered in our experiments, the PLISI would have been reinforced. As such, the implementation of an interactive depression-filling algorithm to infer the lake-water depth (e.g. Berends & Wal, 2016) could be important to implement in ice sheet models to simulate the last deglaciation.

4 Discussion

With a set of model simulations, we have shown that proglacial lakes can greatly influence ice sheet dynamics by providing rapid grounding line retreats. If the magnitude and the timing of this rapid grounding line retreat depends on climate evolution, the instability occurs systematically in the course of the deglaciation as a result of the depressed bedrock resulting from glacial ice load. It is also only weakly sensitive to calving formulation and lake sub-shelf melting rates (supporting information Text S5 and Fig. S9) because of the strongly negative surface mass balance at the NAIS southern margin. In our simulations, the PLISI results in an acceleration of the deglaciation of the

NAIS in its final stage, with rates of volume change of about 2 mSLE per century. The PLISI could be thus responsible of the debated MWP-1B recorded at Barbados (Abdul et al., 2016). Contrary to the MWP-1A, which could be a surface melt response to the abrupt Bølling warming leading to a saddle-collapse (Gregoire et al., 2012), this event is almost entirely mechanically driven although triggered by a decrease in surface mass balance. As such, it is a self-sustained instability that can maintain large ice sheet volume loss regardless of later climate change. The PLISI could explain the fan-like ice streams observed in the geological record at the end of the Younger Dryas (Margold et al., 2018) which also coincide with the MWP-1B.

This mechanism raises a number of scientific questions as we have no contemporaneous analogues, although a large number of glaciers, notably in Patagonia, Greenland and Antarctica, terminate in proglacial lakes (Carrivick & Tweed, 2013). These glaciers are relatively small and do not allow for large floating ice shelves. Instead, the PLISI could have generated large and thick ice shelves floating over freshwater cavities. Since present-day freshwater glaciers show calving and basal melting rates smaller than their tidewater analogues (Benn et al., 2007; Trüssel et al., 2013), large scale sub-shelf refreezing could eventually occur within the cavities. If our experiments are weakly sensitive to calving and sub-shelf melting rates because of the strongly negative surface mass balance at the southern margin of the NAIS during the deglaciation, this might not always be the case for other time periods and/or ice sheets.

If the PLISI mechanism is crucial to understand the deglaciation of the NAIS, it will be as important for the Eurasian ice sheet. Large proglacial lakes were also present at the southern flank of the Eurasian ice sheet, in the vicinity of the Baltic and White seas (Patton et al., 2017). The PLISI could be a mechanism that explains the observed cyclicity in abrupt discharge events recorded in the Black sea (Soulet et al., 2013). More generally, the PLISI could be crucial to understand deglacial Pleistocene eustatic sea level.

While grounding line dynamics is a well established process to account for the Antarctic ice sheet evolution, the PLISI mechanism is another manifestation of its importance for ice sheet dynamics. These results highlight the need for a good understanding of grounding line physics and its representation in numerical models in order to reduce the uncertainties on sea level projections for the ongoing deglaciation.

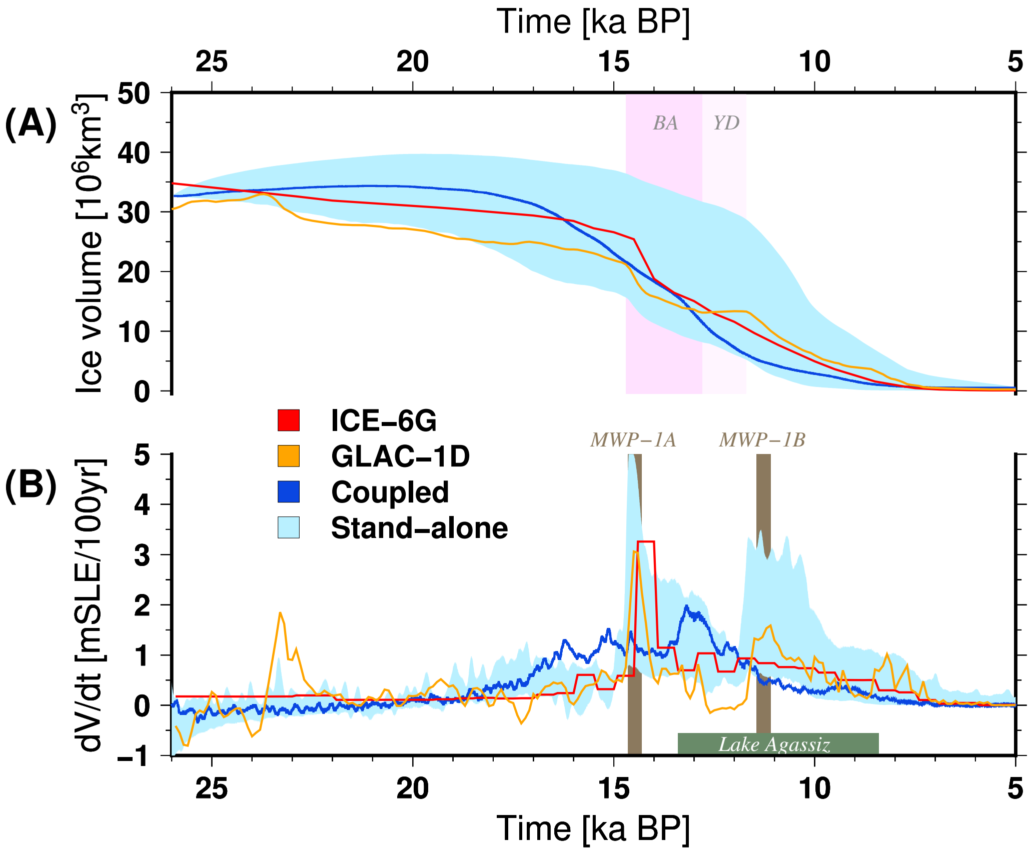

Figure 1. Temporal evolution. Simulated total ice volume (A) and rate of ice loss (expressed as ice volume contributing to sea level rise per century) (B) through the deglaciation (26 kaBP 5 kaBP) for the NAIS. Dark blue depicts the simulated NAIS using the GRISLI-iLOVECLIM set-up while the light blue envelop depicts the spread within the GRISLI stand-alone experiments (Methods). The ice sheet volume and rate of volume change of GLAC-1D and ICE-6G are shown in orange and red, respectively. The Bølling-Allerød warm period and the Younger Dryas cold period are shown by the pink vertical shading. The two melt-water pulses discussed in the text are in brown and the presence of the Lake Agassiz is shown by the horizontal green bar.

Acknowledgments

Archiving of source data of the figures presented in the main text of the manuscript is underway. Data will be made publicly available upon publication of the manuscript on the Zenodo repository with digital object identifier 10.xxxx/zenodo.xxxxxxx. They are temporarily available for review purposes at: https://sharebox.lsce.ipsl.fr/index.php/s/7Aygc0X5Bq3SGx2 (694.9 Mb). The research leading to these results has received funding from the European Research Council under the European Union's Seventh Framework Program (FP7/2007-2013 Grant agreement n 339108).

References

Abdul, N. A., Mortlock, R. A., Wright, J. D., & Fairbanks, R. G. (2016). Younger Dryas sea level and meltwater pulse 1b recorded in Barbados reef crest coral Acropora palmata. *Paleoceanography*, *31*(2), 330–344. doi: 10.1002/2015PA002847

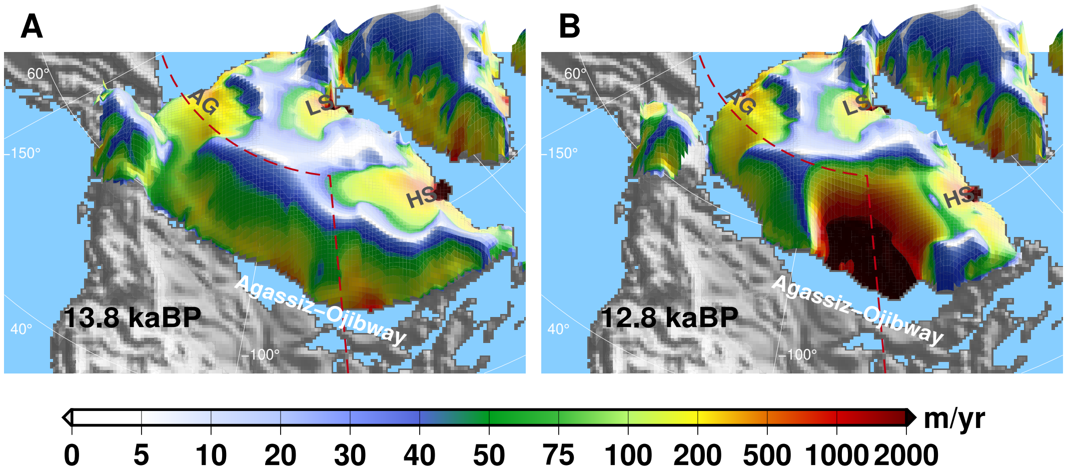

Figure 2. Ice sheet geometry at the time of the instability. Vertically integrated velocity in the coupled experiment for two snapshots, before (A) and after (B) the maximum in rate of ice loss for the NAIS. The two snapshots are separated by one thousand year. For this 3-D perspective plot, the velocity is draped on top of the ice sheet topography. The dashed line stands for the cross-section discussed in the main text. The major simulated ice streams are the Amundsen Gulf (AG), Lancaster Sound (LS) and Hudson Strait (HS) ice streams.

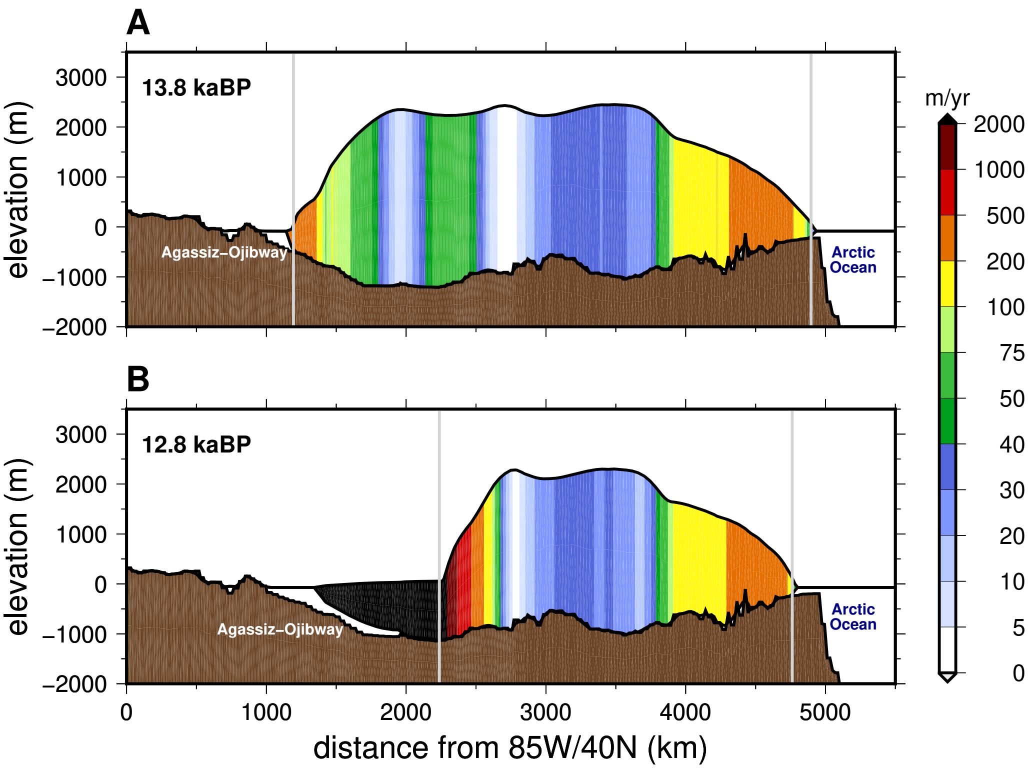

Figure 3. Bedrock profile. Cross-section of the NAIS (dashed line on Fig. 2) in the coupled experiment for two snapshots, before (A) and after (B) the maximum in rate of ice loss. The bedrock is depicted in brown color, the horizontal black line represents the contemporaneous eustatic sea level and the vertically averaged velocity is shown with the color palette. The vertical grey lines represent the position of the grounding line.

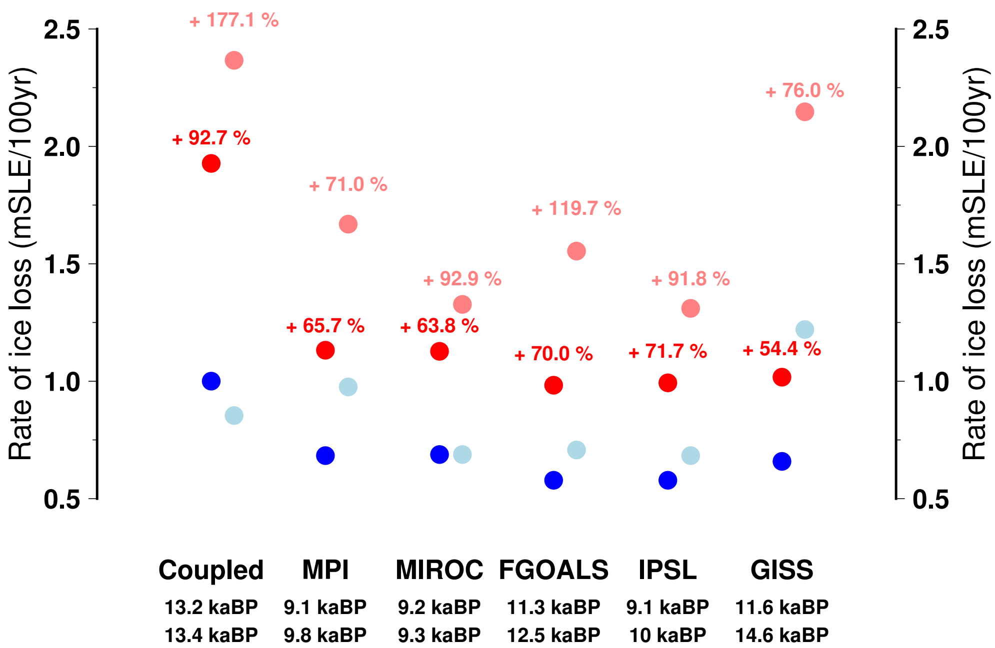

Figure 4. Importance of the lake level for the ice loss. Rate of ice loss towards the maximum of the PLISI event (red dots) and their contemporaneous values when we prevent the PLISI (blue dots) for the coupled model and different stand-alone experiments forced by PMIP3 models (Methods). Light colours represent the experiments in which we assume a lake level higher than the eustatic sea level (prescribed at +50 metres above present-day sea level). Timing of the maximum in rate of ice loss differs for the different lake levels (earlier for higher lake level). The stand-alone experiments here use a weighing factor for the fast variability of 0.25.

Abe-Ouchi, A., Saito, F., Kageyama, M., Braconnot, P., Harrison, S. P., Lambeck, K., … Takahashi, K. (2015, November). Ice-sheet configuration in the CMIP5/PMIP3 Last Glacial Maximum experiments. *Geoscientific Model Development*, *8*(11), 3621–3637. doi: 10.5194/gmd-8-3621-2015

Abe-Ouchi, A., Saito, F., Kawamura, K., Raymo, M. E., Okuno, J., Takahashi, K., & Blatter, H. (2013). Insolation-driven 100,000-year glacial cycles and hysteresis of ice-sheet volume. *Nature*, *500*(7461), 190–193. doi: 10.1038/nature12374

Barber, D. C., Dyke, A., Hillaire-Marcel, C., Jennings, A. E., Andrews, J. T., Kerwin, M. W., … Gagnon, J.-M. (1999, July). Forcing of the cold event of 8,200 years ago by catastrophic drainage of Laurentide lakes. *Nature*, *400*(6742), 344–348. doi: 10.1038/22504

Bard, E., Hamelin, B., Deschamps, P., & Camoin, G. (2016). Comment on "Younger Dryas sea level and meltwater pulse 1b recorded in Barbados reefal crest coral Acropora palmata" by N. A. Abdul et al. *Paleoceanography*, *31*(12), 1603–1608. doi: 10.1002/2016PA002979

Beckmann, A., & Goosse, H. (2003). A parameterization of ice shelfocean interaction for climate models. *Ocean Modelling*, *5*(2), 157–170. doi: 10.1016/S1463-5003(02)00019-7

Benn, D. I., Warren, C. R., & Mottram, R. H. (2007, June). Calving processes and the dynamics of calving glaciers. *Earth-Science Reviews*, *82*(3), 143–179. doi: 10.1016/j.earscirev.2007.02.002

Berends, C. J., & Wal, R. S. W. v. d. (2016, December). A computationally efficient depression-filling algorithm for digital elevation models, applied to proglacial lake drainage. *Geoscientific Model Development*, *9*(12), 4451–4460. doi: 10.5194/gmd-9-4451-2016

Calov, R., Ganopolski, A., Petoukhov, V., Claussen, M., & Greve, R. (2002, December). Large-scale instabilities of the Laurentide ice sheet simulated in a fully coupled climate-system model. *Geophysical Research Letters*, *29*(24), 2216. doi: 10.1029/2002GL016078

Carrivick, J. L., & Tweed, F. S. (2013). Proglacial lakes: character, behaviour and geological importance. *Quaternary Science Reviews*, *78*, 34–52. doi: 10.1016/j.quascirev.2013.07.028

Charbit, S., Kageyama, M., Roche, D., Ritz, C., & Ramstein, G. (2005, October). Investigating the mechanisms leading to the deglaciation of past continental northern hemisphere ice sheets with the CLIMBER GREMLINS coupled model. *Global and Planetary Change*, *48*, 253–273.

Charbit, S., Ritz, C., Philippon, G., Peyaud, V., & Kageyama, M. (2007, January). Numerical reconstructions of the Northern Hemisphere ice sheets through the last glacial-interglacial cycle. *Climate of the Past*, *3*, 15–37.

Clarke, G. K. C., Leverington, D. W., Teller, J. T., & Dyke, A. S. (2004, February). Paleohydraulics of the last outburst flood from glacial Lake Agassiz and the 8200BP cold event. *Quaternary Science Reviews*, *23*(3), 389–407. doi: 10.1016/j.quascirev.2003.06.004

DeConto, R. M., & Pollard, D. (2016). Contribution of Antarctica to past and future sea-level rise. *Nature*, *531*(7596), 591. doi: 10.1038/nature17145

Dee, D. P., Uppala, S. M., Simmons, A. J., Berrisford, P., Poli, P., Kobayashi, S., … Vitart, F. (2011, April). The ERA-Interim reanalysis: configuration and performance of the data assimilation system. *Quarterly Journal of the Royal Meteorological Society*, *137*(656), 553–597. doi: 10.1002/qj.828

Deschamps, P., Durand, N., Bard, E., Hamelin, B., Camoin, G., Thomas, A. L., … Yokoyama, Y. (2012). Ice-sheet collapse and sea-level rise at the Bølling warming 14,600 years ago. *Nature*, *483*(7391), 559. doi: 10.1038/nature10902

Fowler, A. C., Rickaby, R. E. M., & Wolff, E. W. (2013, November). Exploration of a simple model for ice ages. *GEM - International Journal on Geomathematics*, *4*(2), 227–297. doi: 10.1007/s13137-012-0040-7

Ganopolski, A., & Brovkin, V. (2017). Simulation of climate, ice sheets and CO2 evolution during the last four glacial cycles with an Earth system model of intermediate complexity. *Clim. Past*, *13*(12), 1695–1716. doi: 10.5194/cp-13-1695-2017

Gregoire, L. J., Payne, A. J., & Valdes, P. J. (2012). Deglacial rapid sea level rises caused by ice-sheet saddle collapses. *Nature*, *487*(7406), 219. doi: 10.1038/nature11257

Heinemann, M., Timmermann, A., Elison Timm, O., Saito, F., & Abe-Ouchi, A. (2014). Deglacial ice sheet meltdown: orbital pacemaking and CO2 effects. *Clim. Past*, *10*(4), 1567–1579. doi: 10.5194/cp-10-1567-2014

Hostetler, S. W., Bartlein, P. J., Clark, P. U., Small, E. E., & Solomon, A. M. (2000, May). Simulated influences of Lake Agassiz on the climate of central North America 11,000 years ago. *Nature*, *405*(6784), 334–337. doi: 10.1038/35012581

Ivanovic, R. F., Gregoire, L. J., Kageyama, M., Roche, D. M., Valdes, P. J., Burke, A., … Tarasov, L. (2016). Transient climate simulations of the deglaciation 21–9 thousand years before present (version 1) PMIP4 Core experiment design and boundary conditions. *Geoscientific Model Development*, *9*(7), 2563–2587. doi: 10.5194/gmd-9-2563-2016

Krinner, G., Mangerud, J., Jakobsson, M., Crucifix, M., Ritz, C., & Svendsen, J. I. (2004, January). Enhanced ice sheet growth in Eurasia owing to adjacent ice-dammed lakes. *Nature*, *427*(6973), 429–432. doi: 10.1038/nature02233

Lambeck, K., Purcell, A., & Zhao, S. (2017, February). The North American Late Wisconsin ice sheet and mantle viscosity from glacial rebound analyses. *Quaternary Science Reviews*, *158*, 172–210. doi: 10.1016/j.quascirev.2016.11.033

Lambeck, K., Rouby, H., Purcell, A., Sun, Y., & Sambridge, M. (2014). Sea level and global ice volumes from the Last Glacial Maximum to the Holocene. *Proceedings of the National Academy of Sciences*, *111*(43), 15296. doi: 10.1073/pnas.1411762111

Larour, E., Seroussi, H., Morlighem, M., & Rignot, E. (2012, March). Continental scale, high order, high spatial resolution, ice sheet modeling using the Ice Sheet System Model (ISSM). *Journal of Geophysical Research: Earth Surface*, *117*(F1), F01022. doi: 10.1029/2011JF002140

Liu, J., Milne, G. A., Kopp, R. E., Clark, P. U., & Shennan, I. (2016, February). Sea-level constraints on the amplitude and source distribution of Meltwater Pulse 1a. *Nature Geoscience*, *9*(2), 130–134. doi: 10.1038/ngeo2616

MacAyeal, D. R. (1993). Binge/purge oscillations of the Laurentide Ice Sheet as a cause of the North Atlantic's Heinrich events. *Paleoceanography*, *8*(6), 775–784. doi: 10.1029/93PA02200

Margold, M., Stokes, C. R., & Clark, C. D. (2018, June). Reconciling records of ice streaming and ice margin retreat to produce a palaeogeographic reconstruction of the deglaciation of the Laurentide Ice Sheet. *Quaternary Science Reviews*, *189*, 1–30. doi: 10.1016/j.quascirev.2018.03.013

Patton, H., Hubbard, A., Andreassen, K., Auriac, A., Whitehouse, P. L., Stroeven, A. P., … Hall, A. M. (2017, August). Deglaciation of the Eurasian ice sheet complex. *Quaternary Science Reviews*, *169*, 148–172. doi: 10.1016/j.quascirev.2017.05.019

Pattyn, F., Perichon, L., Durand, G., Favier, L., Gagliardini, O., Hindmarsh, R. C. A., … Wilkens, N. (2013). Grounding-line migration in plan-view marine ice-sheet models: results of the ice2sea MISMIP3d intercomparison. *Journal of Glaciology*, *59*(215), 410–422. doi: 10.3189/2013JoG12J129

Peltier, W. R., Argus, D. F., & Drummond, R. (2015). Space geodesy constrains ice age terminal deglaciation: The global ICE-6G_c (VM5a) model. *Journal of Geophysical Research: Solid Earth*, *120*(1), 450–487. doi:

10.1002/2014JB011176
Pollard, D. (1982, March). A simple ice sheet model yields realistic 100 kyr glacial cycles. *Nature*, *296*(5855), 334–338. doi: 10.1038/296334a0
Quiquet, A., Dumas, C., Ritz, C., Peyaud, V., & Roche, D. M. (2018, dec). The GRISLI ice sheet model (version 2.0): calibration and validation for multi-millennial changes of the Antarctic ice sheet. *Geoscientific Model Development*, *11*(12), 5003–5025. doi: 10.5194/gmd-11-5003-2018
Quiquet, A., Roche, D. M., Dumas, C., & Paillard, D. (2018, feb). Online dynamical downscaling of temperature and precipitation within the *i*LOVECLIM model (version 1.1). *Geoscientific Model Development*, *11*(1), 453–466. doi: 10.5194/gmd-11-453-2018
Roche, D. M., Dumas, C., Bügelmayer, M., Charbit, S., & Ritz, C. (2014, July). Adding a dynamical cryosphere to iLOVECLIM (version 1.0): coupling with the GRISLI ice-sheet model. *Geosci. Model Dev.*, *7*(4), 1377–1394. doi: 10.5194/gmd-7-1377-2014
Roche, D. M., Paillard, D., Caley, T., & Waelbroeck, C. (2014, December). LGM hosing approach to Heinrich Event 1: results and perspectives from datamodel integration using water isotopes. *Quaternary Science Reviews*, *106*, 247–261. doi: 10.1016/j.quascirev.2014.07.020
Schoof, C. (2007). Ice sheet grounding line dynamics: Steady states, stability, and hysteresis. *Journal of Geophysical Research (Earth Surface)*, *112*.
Soulet, G., Ménot, G., Bayon, G., Rostek, F., Ponzevera, E., Toucanne, S., … Bard, E. (2013, April). Abrupt drainage cycles of the Fennoscandian Ice Sheet. *Proceedings of the National Academy of Sciences*, *110*(17), 6682–6687. doi: 10.1073/pnas.1214676110
Stuhne, G. R., & Peltier, W. R. (2017). Assimilating the ICE-6G_c Reconstruction of the Latest Quaternary Ice Age Cycle Into Numerical Simulations of the Laurentide and Fennoscandian Ice Sheets. *Journal of Geophysical Research: Earth Surface*, *122*(12), 2324–2347. doi: 10.1002/2017JF004359
Tarasov, L., Dyke, A. S., Neal, R. M., & Peltier, W. R. (2012, January). A data-calibrated distribution of deglacial chronologies for the North American ice complex from glaciological modeling. *Earth and Planetary Science Letters*, *315-316*, 30–40. doi: 10.1016/j.epsl.2011.09.010
Teller, J. T. (1995). History and drainage of large ice-dammed lakes along the Laurentide Ice Sheet. *Quaternary International*, *28*, 83–92. doi: 10.1016/1040-6182(95)00050-S
Teller, J. T. (2003, January). Controls, history, outbursts, and impact of large late-Quaternary proglacial lakes in North America. In *Developments in Quaternary Sciences* (Vol. 1, pp. 45–61). Elsevier. doi: 10.1016/S1571-0866(03)01003-0
Teller, J. T., & Leverington, D. W. (2004, May). Glacial Lake Agassiz: A 5000 yr history of change and its relationship to the δ18O record of Greenland. *GSA Bulletin*, *116*(5-6), 729–742. doi: 10.1130/B25316.1
Trüssel, B. L., Motyka, R. J., Truffer, M., & Larsen, C. F. (2013). Rapid thinning of lake-calving Yakutat Glacier and the collapse of the Yakutat Icefield, southeast Alaska, USA. *Journal of Glaciology*, *59*(213), 149–161. doi: 10.3189/2013J0G12J081
Tsai, V. C., Stewart, A. L., & Thompson, A. F. (2015). Marine ice-sheet profiles and stability under Coulomb basal conditions. *Journal of Glaciology*, *61*(226), 205–215. doi: 10.3189/2015JoG14J221
van den Berg, J., van de Wal, R., & Oerlemans, H. (2008, April). A mass balance model for the Eurasian Ice Sheet for the last 120,000years. *Global and Planetary Change*, *61*(3), 194–208. doi: 10.1016/j.gloplacha.2007.08.015
Weertman, J. (1974). Stability of the Junction of an Ice Sheet and an Ice Shelf. *Journal of Glaciology*, *13*(67), 3–11. doi: 10.3189/S0022143000023327
Wiersma, A. P., & Renssen, H. (2006, January). Modeldata comparison for

the 8.2kaBP event: confirmation of a forcing mechanism by catastrophic drainage of Laurentide Lakes. *Quaternary Science Reviews*, *25*(1), 63–88. doi: 10.1016/j.quascirev.2005.07.009

Winkelmann, R., Martin, M. A., Haseloff, M., Albrecht, T., Bueler, E., Khroulev, C., & Levermann, A. (2011, September). The Potsdam Parallel Ice Sheet Model (PISM-PIK) Part 1: Model description. *The Cryosphere*, *5*(3), 715–726. doi: 10.5194/tc-5-715-2011